

Automatic real-time three-dimensional cell tracking by fluorescence microscopy

G. RABUT & J. ELLENBERG

Gene Expression and Cell Biology/Biophysics Programmes, European Molecular Biology Laboratory, Meyerhofstraße 1, D-69117 Heidelberg, Germany

Key words. 3D imaging, 4D imaging, autofocus, automated microscopy, cell migration, cell tracking, confocal microscopy, fluorescence, mitosis.

Summary

Live cell imaging has become an indispensable technique for cell biologists. However, when grown on coverslip glass used for live cell imaging many cultured cells move even during relatively short observation times and focus can drift as a result of mechanical instabilities and/or temperature fluctuations. Time-lapse imaging therefore requires constant adjustment of the imaging field and focus position to keep the cell of interest centred in the imaged volume. We show here that this limitation can be overcome by tracking cells in a fully automated way using the mass centre of cellular fluorescence. Combined with automated multiple location revisiting, this method dramatically increases the throughput of high-resolution live cell imaging experiments.

Introduction

Within 10 years after the first use of the green fluorescent protein (GFP) in living organisms (Chalfie *et al.*, 1994), live cell fluorescence microscopy has become an indispensable tool for cell biologists. This revolution has led to the development of a wealth of fluorescent reporters suitable for *in vivo* experiments (Zhang *et al.*, 2002; Miyawaki *et al.*, 2003) and was accompanied by a parallel development of fluorescence microscopes (Stephens & Allan, 2003). State-of-the-art laser scanning confocal microscopes, wide-field deconvolution microscopes or multiphoton microscopes have become commercially available to non-specialist biologists allowing them to resolve the three-dimensional (3D) organization of their cells at the limits of optical resolution. These microscopes have been completely motorized to allow full control by the operating software and the user can thus design complex image acquisition protocols, for instance combining time-lapse imaging and photobleaching

to assay protein mobility in living cells (Lippincott-Schwartz *et al.*, 2003). Nevertheless, long-term time-lapse experiments with living mammalian cells currently suffer from a major limitation, i.e. that cells migrate out of the acquisition field within a few hours, requiring frequent manual corrections of the XY stage and Z focus positions. This is a common problem for microscopists imaging live cells as most cultured cells display varying degrees of motility in interphase and even more dramatic changes in cell shape and position during mitosis. Nevertheless, to our knowledge, none of the available operating software programs for commercial microscopes offers a tracking function to keep the cells of interest in focus and centred in the acquisition field.

There are basically two methods to track moving cells with a microscope. Most commonly, images are acquired at a fixed stage and focus position and the movements are analysed afterwards, using an image processing algorithm. This can be a complicated task, especially if many cells/objects are moving within the acquisition field, but many algorithms have been developed to extract motility and/or deformation parameters from the moving cells (Soll, 1995; Miura, 2004). The second possibility, rarely implemented, is to program the microscope to follow the movements of the cell automatically and keep it in the field of view. Such a tracking microscope has been developed by Berg (Berg, 1971; Greene & Barnes, 1977), but it uses a hardware-based tracking method that is not easily portable to other microscopes such as confocal microscopes. We therefore developed a software-based tracking method that can be implemented on any fluorescence microscope with motorized stage and focus. The program determines the 3D mass centre of cellular fluorescence and uses this information to readjust the XYZ position of the microscope. We show here that this is a reliable method that can track cultured mammalian cells and keep them in the acquisition field at high resolution over many hours and days or over an entire cell cycle. Combined with automatic multiple location revisiting it allows high-throughput high-resolution single cell imaging experiments.

Materials and methods

Cell line and culture

To demonstrate the functionality of our 3D tracking macro, we established a normal rat kidney cell line stably expressing histone 2B fused to the red fluorescent protein DiHcRed as described (Daigle *et al.*, 2001; Gerlich *et al.*, 2003). For live cell imaging, cells were cultured in no. 1 LabTekII chambered coverglasses (Nunc) in imaging medium [DMEM with 25 mM HEPES but without phenol red (Gibco) supplemented with 20% FCS and 10 mM glutamine].

Microscope set-up

Live cell images were acquired with a customized LSM510 (Carl Zeiss, Jena, Germany) confocal laser scanning microscope (described in Daigle *et al.*, 2001; Beaudouin *et al.*, 2002). Essential for 3D tracking, it is equipped with an XY-scanning stage and a fast Z-scanning stage (HRZ 200, Zeiss). Cells were imaged using a PlanApochromat 63× DIC 1.4-NA oil-immersion objective and were maintained at 37 °C by an air stream incubator (ASI 400, Nevtek, Burnsville, VA, U.S.A.) in conjunction with an objective heater (Bioptechs, Butler, PA, U.S.A.).

Three-dimensional tracking macro

To track moving cells in real time on our microscope, we developed a 3D tracking macro, written in visual basic for the LSM

2.8 software (Zeiss). The code is available at <http://www.embl-heidelberg.de/ExternalInfo/ellenberg/homepage/macros.html>. Its underlying principle can be ported to other microscope operating software environments that allow users to program applications or macros.

Algorithm

The principle of the tracking algorithm is to measure the movements of the cells to be tracked by analysing the 3D displacements of their fluorescence mass centre. The flow chart of the macro algorithm is shown schematically in Fig. 1(A). Its core consists of two modules for 3D tracking and image acquisition.

Three-dimensional tracking module. The 3D tracking module starts at the latest known XYZ position of the tracked cell. A series of XY fluorescence images is acquired at a Z-range around the current focus position, resulting in a 3D dataset (Fig. 2A). The distances between the centre of the imaged volume and mass centre of the tracked cell are then calculated for each axis.

For example, to calculate D_x , this distance along the X-axis, the intensities $I_{x,y,z}$ of all voxels from any YZ plane are summed (S_x , Eq. 1) to obtain a 1D map of the fluorescence intensity distribution in the X direction (Fig. 2Bx, 2Cx):

$$S_x = \sum_{y,z} I_{x,y,z} \quad (1)$$

The projected intensity values S_x are then thresholded (T_x , Eq. 2) to set the background intensity to 0:

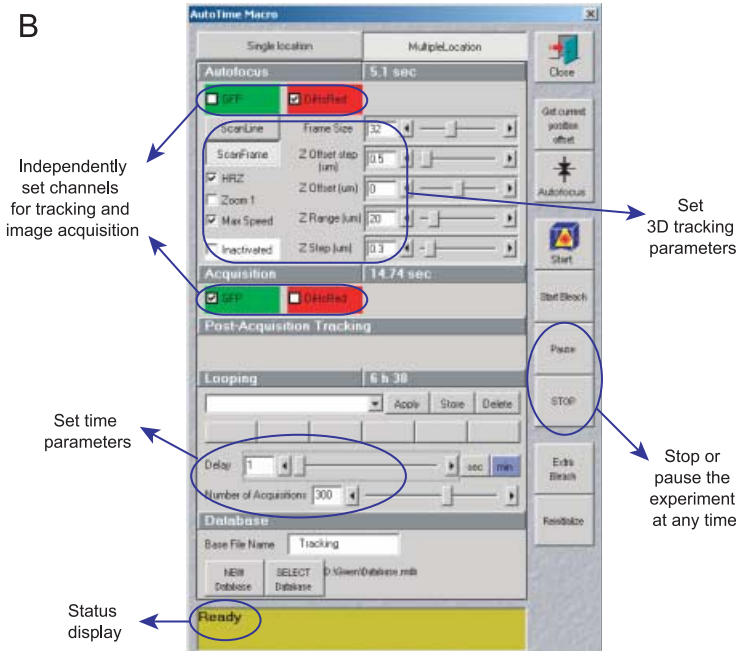
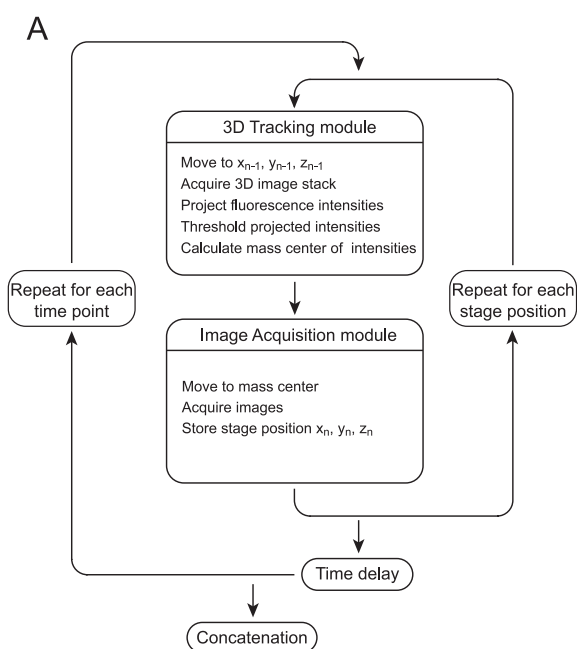


Fig. 1. Flow chart of the 3D tracking macro algorithm (A) and the main features of the user interface (B).

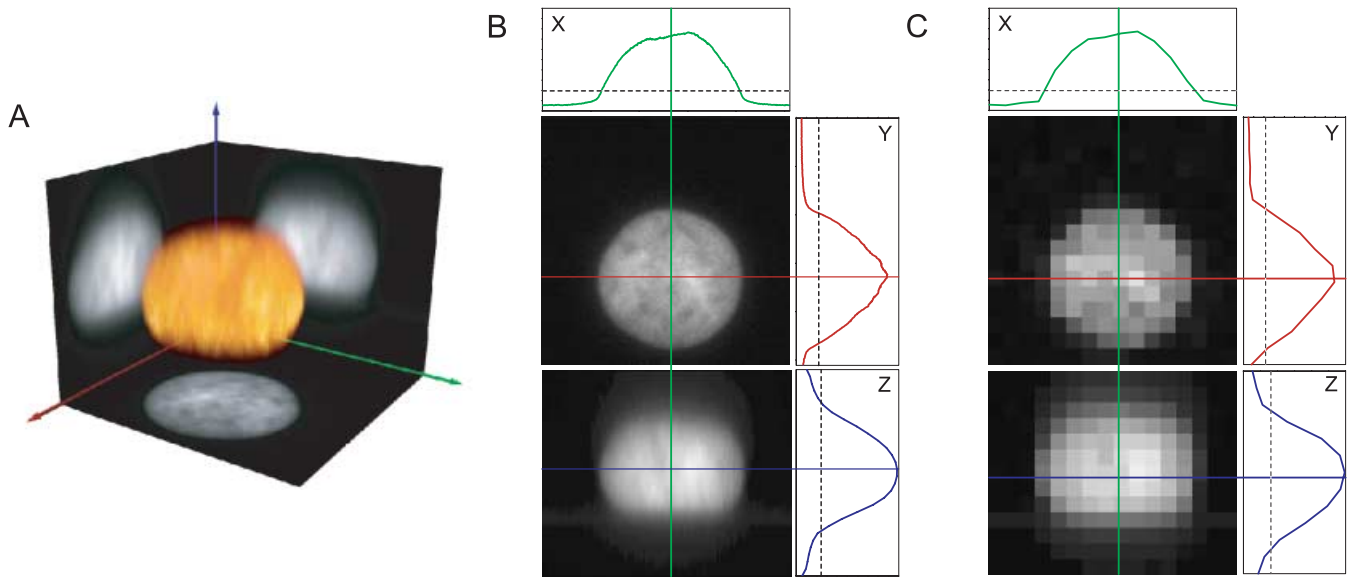


Fig. 2. The 3D tracking module acquires a 3D dataset of fluorescence images (A) and calculates 1D fluorescence intensity profiles along the X, Y and Z axes (B and C) to map the position of the mass centre of the fluorescence intensity (continuous lines). The dotted lines indicate the thresholds that were used to calculate the position of the mass centre of fluorescence intensity (see Materials and methods). Even coarse images containing very few pixels (C) are sufficient for accurate determination of the 3D position of the fluorescence intensity mass centre (compare B and C).

$$T_x = \frac{(S_x - \text{thres}_x) + |S_x - \text{thres}_x|}{2} \quad (2)$$

The threshold thres_x (dotted line in Fig. 2B,C) was set at the minimum value of S_x plus 20% of the difference between the maximum and minimum values of S_x , as shown in Eq. (3):

$$\text{thres}_x = \min(S_x) + 0.2 \times (\max(S_x) - \min(S_x)). \quad (3)$$

Finally, D_x is calculated as the distance between the centre of the imaged volume and the mass centre of the thresholded projected intensities T_x along the X axis:

$$D_x = \frac{\sum_x (T_x \times d_x)}{\sum_x T_x} \quad (4)$$

where d_x is the distance (positive or negative) between a pixel x and the centre of the images along the X axis. Equation (5) indicates how to obtain d_x knowing v_x , the voxel size and x_{\max} , the number of pixels along the X axis:

$$d_x = \left(x - \frac{x_{\max} + 1}{2} \right) \times v_x \quad (5)$$

D_y and D_z are subsequently obtained in an analogous manner.

Image acquisition module. After completion of the 3D tracking module, the stage and focus are moved to the determined 3D position of the centre of mass of the tracked cell. An XY image

or a series of images (in Z or t) is then acquired at this position and saved. The position coordinates are updated for the next cycle and stored in a spreadsheet file for later analysis of cell movement in 3D.

Looping. The 3D tracking and image acquisition modules are looped at two different levels (Fig. 1A). First, the user can define multiple stage positions from where to acquire images of single cells. Each position is visited sequentially and tracked individually. Once all stored stage positions have been visited the whole procedure is repeated as many times as needed. The time-lapse of image acquisition at a given stage position is limited by the time required to track and image each location and move between locations. To reduce image acquisition frequency, the user can set the time-lapse longer by defining a time delay before each time repetition (Fig. 1A). A typical example for mammalian cells is to image 20 cells at different locations, imaged in 15 Z-slices every 10 min (Fig. 3C).

User interface

We designed the user interface (Fig. 1B) to achieve three major goals. First, we wanted user friendliness for fast and intuitive experimental design. All command and parameter settings required to execute the macro are accessible from a single window (Fig. 1B). Other more general parameters, such as image settings, are set normally in the core microscope software (here Zeiss LSM 2.8). A status bar informs the user of the actions being performed by the macro at any time.

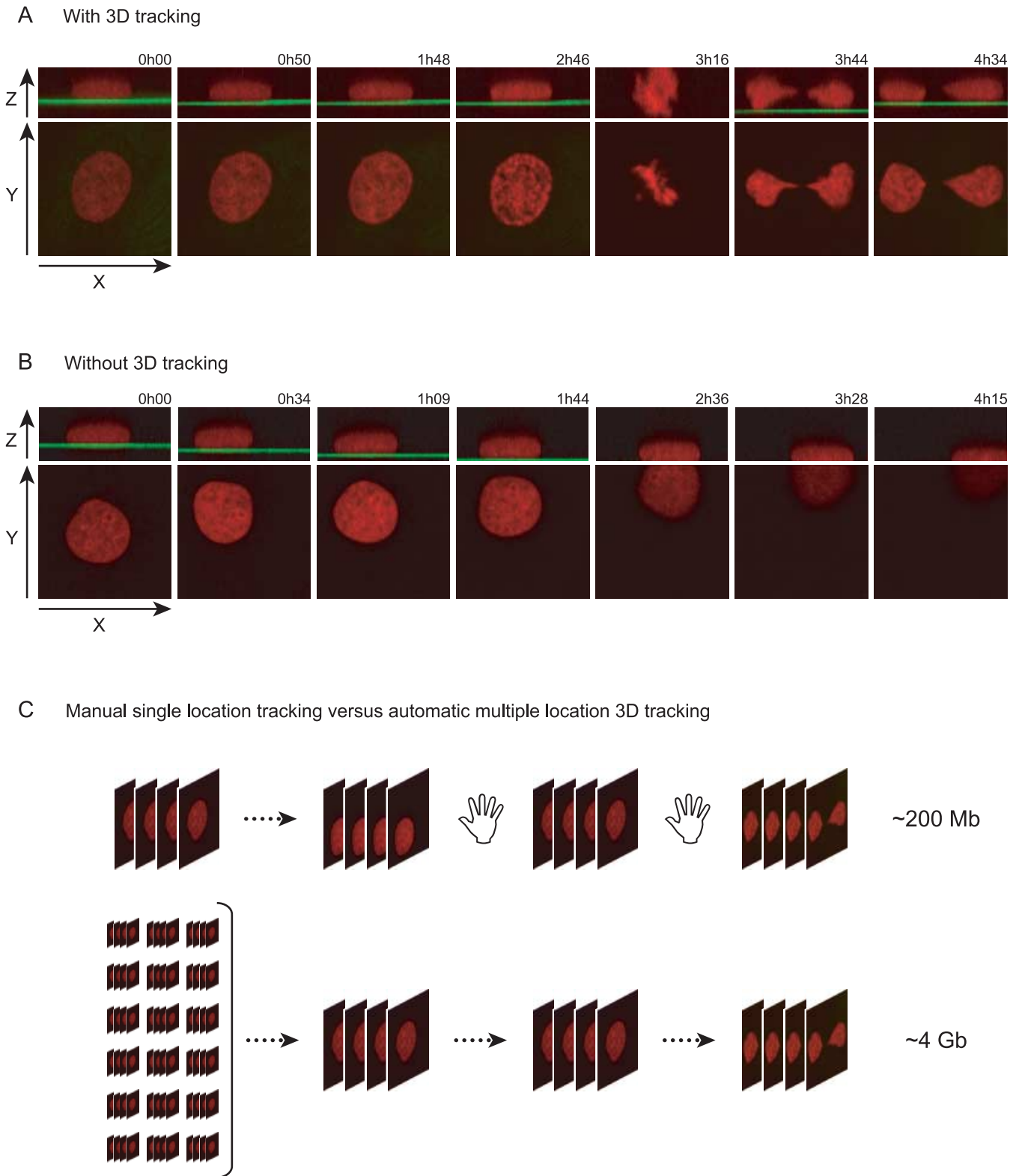


Fig. 3. Three-dimensional image stacks of NRK cells expressing H2B-DiHcRed (red) were acquired for several hours. To monitor the focus position changes, a second channel (green) was configured to image the laser reflection at the interface between the coverslip and the imaging medium (green). Without 3D tracking (B) the cell moves out of the imaged field and goes out of focus. When the 3D tracking macro is used (A) the stage and focus positions are modified before every image acquisition to keep the cell in the centre of the imaged volume. (C) Combined with multiple location imaging the 3D tracking macro allows automatic parallel long-term 3D time-lapse experiments.

Our second goal was flexibility so that the user can interactively design complex experiments. Different channels for 3D tracking and image acquisition can be defined. Thus a reference channel (e.g. Hoechst 33342 DNA vital stain; H2B-DiHcRed) can be used for tracking to prevent unnecessary illumination in the imaging channel (e.g. GFP). Images can be acquired at a given offset above or below the determined mass centre position along the Z axis if the user decides, for instance, to image only the top or the bottom of the cell. In addition, the macro can be stopped or paused at any time during the experiment and its parameters modified interactively. This is extremely useful to optimize parameters or react to changes in cell morphology and/or dynamics without terminating the time-lapse experiment.

The third goal was speed and robustness. To minimize the time required for the 3D tracking module, the user can choose to use the maximum available scan speed and reduce the number of pixels in X and Y as well as the frame spacing and the range to be scanned in Z. In our experience, even very coarse and fast tracking scans, for instance $16 \times 16 \times 16$ pixels, are more than sufficient to map precisely the fluorescence mass centre of the cell (Fig. 2C). Finally, the optional use of a fast focusing Z-scanning stage or a piezo stepper to focus the objective (Hammond & Glick, 2000) drastically reduces the acquisition time of 3D stacks. Combining these features, the 3D tracking module can be reduced to ~ 2 s per location and is therefore not limiting for most long-term experiments that typically last many hours or even days. For robustness, the macro automatically saves the image files in a database, one by one immediately following their acquisition at each location. This reduces demands on computer memory and avoids any data loss in case of a user mistake, power cut or software crash. However, the experiments can typically not be restarted after a crash as the current version of the LSM software does not enable the user to store or load stage and focus positions.

Concatenation of individual images into a timeseries

Because all the image files are stored individually following their acquisition at each timepoint for each location, the user needs to concatenate them into a multidimensional timeseries for data browsing and analysis. Concatenation needs to be automated to handle the large amounts of data generated by multilocation 3D tracking. We therefore developed a concatenation macro that automatically generates timeseries files for each stage position and preserves the image metadata such as acquisition timestamps, voxel sizes, etc.

Results and discussion

We show here that the mass centre of cellular fluorescence intensity distribution can efficiently be used to determine the position of moving cells (see Figs 2 and 3). The mass centre algorithm is simple to program and can be calculated rapidly.

Importantly, the determination of mass centre position is also accurate in very low-resolution images compared with full-resolution images (compare panels B and C in Fig. 2). Thus rapidly scanned coarsely sampled 3D images are sufficient for the tracking module, drastically reducing the time required for tracking. However, using the fluorescence mass centre requires that the imaging field contains only a single fluorescent cell. If a second cell enters the imaging field or if the tracked cell divides during the experiment, the microscope will centre the imaging field between the two cells (see Fig. 3A). As the two cells will move in an uncoordinated fashion, one cell may move out of the imaging field and the microscope will then keep tracking the other one. For efficient tracking, cells should thus be grown at a relatively low density ($\sim 10\,000$ cells cm^{-2} here). Alternatively, neighbouring fluorescent cells can be completely photobleached in the tracking channel before starting the macro.

As an example, we show that our tracking macro can accurately and reliably track moving mammalian cells expressing a fluorescent nuclear marker protein such as H2B-DiHcRed (Fig. 3). Similar tracking fidelity was achieved also with other fluorescence markers such as cytoplasmic GFP (data not shown). In cases where the fluorescence signal of interest for high-resolution imaging is not suitable for tracking because of very poor signal, separate channels for tracking (using a bright vital counterstain such as Hoechst 33342 or a fluorescent protein of different colour) and for image acquisition can be used (Fig. 2B). Finally, because the fluorescence mass centre enables the user to track the cells in three dimensions it can be used to follow systematic cell movements in Z as they occur, e.g. during mitosis of adherent cells (Fig. 3A), or to correct focus fluctuations (Fig. 3B) resulting from focus wheel/stage drifts (Burglin, 2000) or temperature fluctuations in the microscope room.

The tracking macro allows the user to acquire images of a single moving cell at least once every 5 s. It is thus possible to track cells moving up to $50\ \mu\text{m}$ within 5 s even when using a high-magnification $63\times$ oil-immersion objective (field of view $\sim 200\ \mu\text{m}$). This is more than sufficient to study even highly motile cells, such as *Dictyostelium discoideum* or goldfish keratocytes that all have maximum instantaneous velocities below $50\ \mu\text{m}\ \text{min}^{-1}$ (Euteneuer & Schliwa, 1984; Chubb *et al.*, 2002). Our 3D tracking macro therefore makes it now possible to study the migration of single cells over long distances, which might reveal long-term migratory properties overlooked in short-term studies. To analyse the properties of cell migration, the tracking macro stores the 3D position of the cell at each time point. As an example, Fig. 4 displays the relative movements of five cells tracked over 17 h. Other parameters such as instantaneous speed, direction of movement, the frequency of speed or directions changes (Soll, 1995) can readily be calculated from these tracks.

Besides cell migration, imaging the entire cell volume at high resolution during the dramatic lateral and axial movements

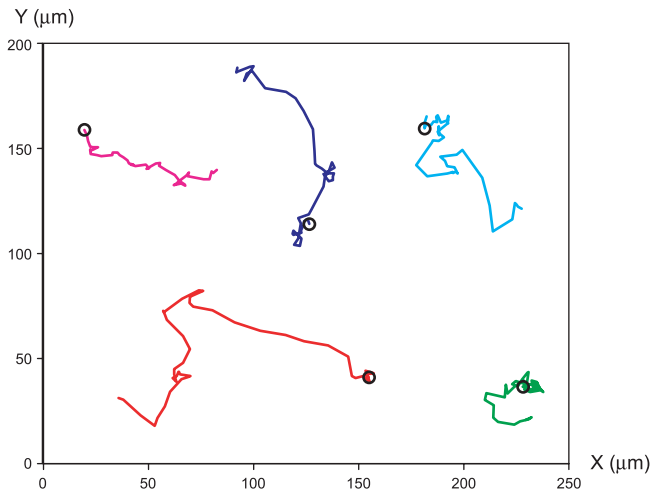


Fig. 4. Relative XY coordinates of five cells expressing H2B-DiHcRed tracked over 17 h with the 3D tracking macro. Circles indicate initial cell positions.

that occur during mitosis is a good example of the power of the tracking macro (Fig. 3A). A typical adherent mammalian fibroblast changes from a flat 5- μm -high object to a spherical 20- μm -high object in mitosis and flattens again after chromosome segregation followed by migration of the daughter cells. Our macro makes it possible to observe the entire cell volume during a full cell cycle with high resolution in a fully automated way. Thus studying the dynamic changes in protein localization during the cell cycle is easily feasible in high throughput. Similarly, changes of cell morphology over long times are observed in many biological processes, such as during bacterial or viral infections (see for instance Gallego-Gomez *et al.*, 2003) and those processes can thus be imaged automatically with the macro. More generally, the macro permits the user reliably to image cellular processes happening over several hours or days that would be very laborious to study otherwise. For instance, we recently dissected the dynamic organization of the very stable nuclear pore complexes using this macro (G. Rabut *et al.*, unpublished data), the disassembly and reassembly of the nucleolus (Leung *et al.*, 2004) and the condensation and segregation of chromosomes (D. Gerlich and J. Ellenberg, unpublished data).

It is of course possible to run 3D tracking time-lapse imaging experiments in parallel, by tracking multiple cells at different locations sequentially (Figs 3C and 4). We routinely use the macro to track 20 cells during one 12-h experiment, but more cells can be tracked, the main limitation being the time needed for the initial cell selection and the time required to revisit all individual positions. This allows us to monitor many potentially interesting cells in parallel and even under different physiological conditions when using multiwell chambers. Automatic multilocation tracking time-lapse dramatically increases the single cell experiment throughput, especially useful when the observed processes are slow and/or rare.

Parallel tracking rapidly generates large amounts of data (tens of gigabytes per experiment), especially if multicolour 3D datasets are acquired. Post-acquisition image processing and analysis (Gerlich & Ellenberg, 2003), which are still poorly automated, then become the bottleneck of the experimental throughput.

Conclusion

We show here that multilocation 3D tracking functions not available on current commercial fluorescence microscopes can be easily implemented as an add-in. When working with living cells, such a tool opens up a wide range of possible long-term imaging experiments. Multiple cells can be automatically imaged in parallel over tens of hours, which would be extremely time consuming to perform manually. Our method thus allows high-resolution single cell time-lapse imaging to be used as a reliable and robust microscopy screening assay to study, for example, the cell cycle, cell migration or the development of loss-of-function phenotypes in RNAi experiments. Importantly, any fluorescence microscope with motorized stage and focus can use the described method. In addition to increasing throughput and reducing hands-on time, it also allows using the microscope time most efficiently, for instance by planning long-term experiments during overnight and/or weekend slots.

Acknowledgements

We would like to thank Nathalie Daigle for the H2B-DiHcRed stable cell line. Richard Ankerhold at Carl Zeiss Jena helped by providing the codes of example macros and providing information on the LSM 5 macro interface. J.E. acknowledges support from the German Research Council (DFG, EL 246/1-1) and the Human Frontiers Science Program (RGP0031/2001-M).

References

- Beaudouin, J., Gerlich, D., Daigle, N., Eils, R. & Ellenberg, J. (2002) Nuclear envelope breakdown proceeds by microtubule-induced tearing of the lamina. *Cell*, **108**, 83–96.
- Berg, H.C. (1971) How to track bacteria. *Rev. Sci. Instrum.* **42**, 868–871.
- Burglin, T.R. (2000) A two-channel four-dimensional image recording and viewing system with automatic drift correction. *J. Microsc.* **200**, 75–80.
- Chalfie, M., Tu, Y., Euskirchen, G., Ward, W.W. & Prasher, D.C. (1994) Green fluorescent protein as a marker for gene expression. *Science*, **263**, 802–805.
- Chubb, J.R., Wilkins, A., Wessels, D.J., Soll, D.R. & Insall, R.H. (2002) *Pseudopodium* dynamics and rapid cell movement in *Dictyostelium* Ras pathway mutants. *Cell Motil. Cytoskeleton*, **53**, 150–162.
- Daigle, N., Beaudouin, J., Hartnell, L., Imreh, G., Hallberg, E., Lippincott-Schwartz, J. & Ellenberg, J. (2001) Nuclear pore complexes form immobile networks and have a very low turnover in live mammalian cells. *J. Cell Biol.* **154**, 71–84.

- Euteneuer, U. & Schliwa, M. (1984) Persistent, directional motility of cells and cytoplasmic fragments in the absence of microtubules. *Nature*, **310**, 58–61.
- Galleo-Gomez, J.C., Risco, C., Rodriguez, D., Cabezas, P., Guerra, S., Carrascosa, J.L. & Esteban, M. (2003) Differences in virus-induced cell morphology and in virus maturation between MVA and other strains (WR, Ankara, and NYCBH) of vaccinia virus in infected human cells. *J. Virol.* **77**, 10606–10622.
- Gerlich, D., Beaudouin, J., Kalbfuss, B., Daigle, N., Eils, R. & Ellenberg, J. (2003) Global chromosome positions are transmitted through mitosis in mammalian cells. *Cell*, **112**, 751–764.
- Gerlich, D. & Ellenberg, J. (2003) 4D imaging to assay complex dynamics in live specimens. *Nat. Cell Biol.* **5** (Suppl.), S14–19.
- Greene, F.M. Jr & Barnes, F.S. (1977) System for automatically tracking white blood cells. *Rev. Sci. Instrum.* **48**, 602–604.
- Hammond, A.T. & Glick, B.S. (2000) Raising the speed limits for 4D fluorescence microscopy. *Traffic*, **1**, 935–940.
- Leung, A.K.L., Gerlich, D., Miller, G. *et al.* (2004) Quantitative kinetic analysis of nucleolar breakdown and reassembly during mitosis in live human cells. *J. Cell Biol.* **166**, in press.
- Lippincott-Schwartz, J., Altan-Bonnet, N. & Patterson, G.H. (2003) Photo-bleaching and photoactivation: following protein dynamics in living cells. *Nat. Cell Biol.* **00** (Suppl.), S7–14.
- Miura, K. (2004) Tracking movement in cell biology. *Advances in Biochemical Engineering/Biotechnology* (ed by J. Rietdorf). Springer Verlag, Berlin, in press.
- Miyawaki, A., Sawano, A. & Kogure, T. (2003) Lighting up cells: labelling proteins with fluorophores. *Nat. Cell Biol.* **00** (Suppl.), S1–7.
- Soll, D.R. (1995) The use of computers in understanding how animal cells crawl. *Int. Rev. Cytol.* **163**, 43–104.
- Stephens, D.J. & Allan, V.J. (2003) Light microscopy techniques for live cell imaging. *Science*, **300**, 82–86.
- Zhang, J., Campbell, R.E., Ting, A.Y. & Tsien, R.Y. (2002) Creating new fluorescent probes for cell biology. *Nat. Rev. Mol. Cell Biol.* **3**, 906–918.